COMMUNICATIONS IN SCIENCE AND TECHNOLOGY
Homepage: cst.kipmi.or.id

Investigating the impact of nanoparticle geothermal silica loading on the mechanical properties and vulcanization characteristics of rubber composites

Muh. Wahyu Sya'bani[a,b,*], Rochmadi[a], Indra Perdana[a], Agus Prasetya[a]

[a]*Department of Chemical Engineering, Universitas Gadjah Mada, Yogyakarta 55281, Indonesia*
[b]*Department of Rubber and Plastic Processing Technology, Politeknik ATK Yogyakarta, Yogyakarta 55187, Indonesia*

Article history:
Received: 26 May 2023 / Received in revised form: 18 June 2023 / Accepted: 21 June 2023

Abstract

The present study investigates the effects of nanoparticle geothermal silica (NGS) on the mechanical properties and vulcanization characteristics of rubber compounds with various filler loadings. The rubber compounds were filled with 0, 20, 30, and 40 phr of silica. The properties of NGS were analyzed using transmission electron microscopy, particle size analyzer, and BET surface area analysis to examine its morphology, size distribution, and surface area. The mechanical properties and vulcanization characteristics of the rubber compounds reinforced with NGS were evaluated using a universal testing machine and moving die rheometer. The results showed that NGS possessed the primary particle sizes below 20 nm and a surface area of 168.35 m^2/g. The interaction between silica and rubber determined the modulus of the rubber composites and the vulcanization characteristics. The tensile strength of the rubber compounds, meanwhile, showed a significant increase more than threefold as the filler loading increased from 0 phr to 30 phr, followed by a slight decline at 40 phr loading. The addition of 20 phr of silica led to a prolonged scorch time compared to the filler-free compound due to the adsorption of activators and accelerators. However, the scorch time decreased after reaching 30 phr of silica loading, which could be attributed to the higher amount of bound rubber covering a portion of the silica surface, thereby reducing its ability to adsorb the activator. The presence of silica with good thermal conductivity enabled a better heat transfer during the vulcanization process, resulting in shorter curing times for higher loading. Rubber compounds with an NGS loading of 30 phr demonstrated a favorable balance between filler-rubber interactions, vulcanization characteristics, and mechanical properties in the rubber compounds.

Keywords: Geothermal waste; rubber; silica nanoparticle; vulcanization; mechanical properties

1. Introduction

Utilizing water vapor from geothermal sources offers a sustainable and renewable energy source [1]. However, there is a challenge for geothermal power plants, silica scaling in pipelines leads to a decline in operational efficiency [2,3]. Commonly, the methods to address this issue generate significant silica sludge, typically disposed of in landfills [4]. The silica content in the sludge is notably high, ranging from 50% to 98% [1,3,5]. Hence, geothermal solid waste shows potential as a viable source of silica raw materials.

Silica, which is composed of silicon dioxide (SiO_2), is a versatile functional material utilized to enhance the surfaces and mechanical characteristics of various materials [6]. The use of silica sludge as a rubber filler is particularly intriguing since over 50% of precipitated silica is utilized in the rubber industry. One of the industries that extensively use silica is the tire manufacturing sector, where fillers account for 30-50% of the composition [7,8]. Adding silica to tire compounds can enhance the properties of rubber vulcanizations, including tensile strength, elongation at break, tear strength, and heat aging resistance [9,10]. Compared to the use of carbon black filler, it is observed that silica decreases rolling resistance, thereby offering the potential for lowering vehicle emissions and fuel consumption [10,11].

Previous research has explored the use of geothermal sludge as a filler in rubber products. However, the quality of the silica particles obtained from the sludge has not reached the level of commercially available silica specifically designed for rubber applications [3,9]. As a consequence, the properties of the final rubber product are negatively affected. Hence, untreated silica from geothermal sludge is only suitable for rubber products that do not require high mechanical properties [9]. In our previous study, we successfully synthesized precipitated nanoparticle silica from geothermal sludge with a purity of 99.01% and an amorphous structure [12]. Hence, further investigation is necessary to determine the potential of silica as a reinforcing filler in rubber.

The amount of filler added also contributes to modifying the curing characteristics of the compound through its interaction with the other compounding ingredients [10]. Additionally, the dispersion of silica within the rubber matrix and the interaction between the polymer and filler impact the product's physical

* Corresponding author.
Email: mwsyabani@atk.ac.id
https://doi.org/10.21924/cst.8.1.2023.1190

properties [13]. Therefore, the objective of this study is to examine the impacts of silica loading on the characteristics of the rubber composite.

2. Materials and Methods

In this research, several instruments were utilized to analyze the influence of incorporating geothermal silica nanoparticles into rubber compounds. The details of the materials and methods adopted can be observed in the following section.

2.1. Materials

The synthesis of geothermal silica nanoparticles used geothermal sludge (PT. Geodipa Energy, Indonesia), sodium hydroxide (Merck, Germany), and sulfuric acid (Merck, Germany). The rubber compounds utilized in the study consisted of the following materials: natural rubber (SIR 3L, Indonesia), styrene-butadiene rubber (Indopol 1502, Indonesia), polybutadiene rubber (LG Chemical BR 1280, China), paraffinic oil (Pertamina P-60, Indonesia), polyethylene glycol (PEG4000, China), zinc oxide (Indolysaght ZnO, Indonesia), stearic acid (SA 1801, Indonesia), mercaptobenzothiazole (Sunsine MBT, China), 2-mercaptobenzothiazole disulfide (Zhedong MBTS, China), tetramethyl thiuram disulfide (Kemai TMTD, China), and sulfur (Indosulfur Mitrakimia, Indonesia).

Table 1 provides the detailed information on the composition of the rubber compound.

Table 1. Rubber composite formulation

Materials	Amount (phr*)
NR	35.0
SBR	35.0
BR	30.0
Silica	0/20.0/30.0/40.0
Paraffinic Oil	2.0
Polyethylene Glycol	3.0
Zinc Oxide	5.0
Stearic Acid	1.0
MBT	1.0
MBTS	1.0
TMTD	0.5
Sulfur	2.5

*phr, parts per hundred rubber by weight

2.2. Preparation of nanoparticle geothermal silica

The synthesis of precipitated nanoparticle geothermal silica was carried out using the methods as described in our previous work [12]. The geothermal sludge underwent a two-step washing procedure using hot water dan sulfuric acid at 90°C. Afterward, the purified geothermal silica was washed and dried. 40 grams of purified silica were combined with 260 mL of 13%NaOH and boiled for 2 hours to form a slurry solution. The solution was then filtered to eliminate impurities, resulting in a sodium silicate solution.

To obtain the primary solution, the sodium silicate solution underwent two rounds of dilution, and the resulting solution was further diluted twice to obtain the secondary solution. Subsequently, the acid solution (3% H_2SO_4) was added gradually to the 500 mL primary sodium silicate solution for 30 minutes until reaching the desired pH value. The subsequent step involved the modification of the silica structure by utilizing soluble silica and the Ostwald ripening mechanism and by simultaneously adding a 1000 mL secondary sodium silicate solution and 9% sulfuric acid to maintain the pH value. The precipitated silica was washed and dried at 100°C for 24 hours, resulting in the nanoparticle geothermal silica (NGS).

2.3. Preparation of the rubber compounds

The compounding process comprises two stages: mastication and masterbatch mixing. During the mastication stage, 100 parts per hundred rubber (phr) rubber were placed on a two-roll mill (Qingdao Rubber Machinery XK-560) and processed until reaching a soft consistency. Subsequently, additional materials, excluding the vulcanization materials (referred to as masterbatch I), were introduced and thoroughly mixed until being homogenous. Following this, vulcanization additives (masterbatch II) were incorporated to produce rubber compound sheets. The thickness of the resulting sheets was then adjusted using calendaring. Table 2 presents the detailed mixing procedures for compounding.

Table 2. Mixing procedure of rubber compounds

Order	Action	Time (min)
1	Mastication (NR, SBR, BR)	5
2	Mixing Masterbatch I (Silica, Paraffinic Oil, BHT, PEG, ZnO, Stearic Acid)	10
3	Mixing Masterbatch II (MBT, MBTS, TMTD, Sulfur)	5
4	Sheeting	2
		22

2.4. Geothermal silica nanoparticle characterization

To examine silica morphology, Transmission Electron Microscopy (JEOL JEM-1400) was employed, while the surface area was determined using a BET Surface Area Analyzer (Quantachrome Nova 2000). The aggregate size of silica was analyzed using a Particle Size Analyzer (Horiba Scientific SZ-100). The dispersion of silica into the rubber matrix was analyzed using a Scanning Electron Microscope (Thermo Fischer Phenom SEM)

2.5. Rubber composites properties

2.5.1. Bound rubber content

The calculation of bound rubber content (BRC) involved immersing 0.2 grams of the rubber compound in 50 ml of toluene for seven days at room temperature, both in a standard environment and an ammonia environment [14]. Following the seven-day immersion, the sample was dried and weighed. The BRC (%) was determined by employing Equation (1).

$$BRC(\%) = \left(\frac{W_1 - W_2}{W_o \, x \, \frac{100}{W_3}}\right) \quad (1)$$

In the provided equation, wo, w_1, and w_2 represent the weights of the initial sample, dried extracted sample, and insoluble material, respectively. Meanwhile, w_3 denotes the total compound expressed in parts per hundred. The determination of the total bound rubber content (BRC) was carried out under normal environmental conditions. However, since ammonia disrupted the physical bond between the rubber and filler, the chemical BRC was measured in the presence of ammonia. The physical BRC was then calculated as a difference between the total BRC and the chemical BRC.

2.5.2. Swelling and crosslink density

The apparent crosslink density was determined by immersing a 0.2-gram sample of the vulcanized rubber in 50 ml of toluene at room temperature for 72 hours. The solvent was then refreshed after 24 hours. Afterward, the samples were dried for 24 hours at room temperature and re-weighed.

The swelling value, denoted as Q, is defined as the ratio of grams of toluene per gram of rubber hydrocarbon. It was calculated using Equation (2), as specified in reference [14].

$$Q = \left(\frac{W_1 - W_2}{W_0}\right) x \, \frac{W_3}{100} \quad (2)$$

In the given equation, wo, w_1, and w_2 represent the weights of the initial, swollen, and dried samples, respectively. On the other hand, w_3 signifies the total formula weight per hundred rubbers (phr). The obtained swelling results were utilized to compute the molecular weight between the crosslinks (Mc) using the Flory-Rehner equation [15].

$$Mc = \frac{-\rho_p V_s {V_r}^{1/3}}{\ln(1-V_r) + V_r + \chi {V_r}^2} \quad (3)$$

$$V_r = \frac{1}{1+Q_m} \quad (4)$$

The equation incorporates several variables in which ρ represents the density of the rubber, Vs were the molar volume of the solvent, and Vr were the volume fraction of the rubber in the swollen sample. Qm represents the weight increase of the sample in the solvent, while χ is an interaction parameter characterizing an interaction between the rubber network and the solvent. In this study, three different types of rubber were employed, necessitating the correction of parameter values using the Rani methods [16]. The degree of crosslink density can be calculated using Equation (5).

$$V_c = \frac{1}{2M_c} \quad (5)$$

2.5.3. Curing characteristics

The curing characteristics were determined using the moving dies rheometer (Gotech MDR GT-M2000) in accordance with ASTM D2084-01. The vulcanization process was done at a temperature of 150°C.

2.5.4. Mechanical properties

The mechanical properties of the vulcanized rubber were assessed by ASTM D412-06 using dumbbell-shaped samples and a universal testing machine (Gester GT-K01). To prepare the samples, a thickness of 2 mm was achieved through compression molding at a temperature of 150°C and a pressure of 100 bar according to the rheometer test result. Hardness measurements were conducted using a durometer shore A, following the guidelines outlined in ASTM D2240.

3. Results and Discussion

3.1. Silica characterization

White powder NGS was produced using the sol-precipitation technique to create silica aggregates. Soluble silica was generated by introducing secondary sodium silicate and sulfuric acid simultaneously, reinforcing the existing aggregates through the Oswald ripening mechanism. The morphology of NGS was examined using transmission electron microscopy (TEM) as illustrated in Figure (1).

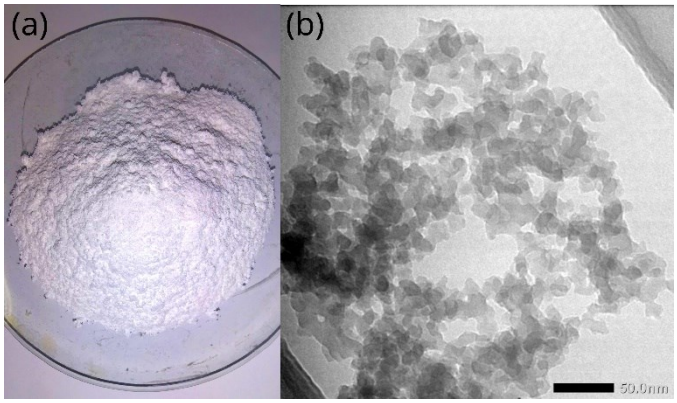

Fig. 1 Geothermal silica nanoparticle (a) powder and (b) TEM 80.000x

In this method, a constant supply of soluble silica within the reactor tended to condense onto the existing aggregate due to the thermodynamic preference for this process over the formation of new nuclei [17]. This condensation occurred at the point of lowest solubility, which typically occurs at the junction between particles [18]. Thus, the reinforcement of the silica aggregates, as shown in Figure 1(b), occurred. The integrity of the silica structure during the drying phase is essential since weak aggregates can collapse under the influence of water tension during drying, leading to the formation of dense and rigid silica particles [19,20]. Incorporating such hard silica in rubber compounding is unfavorable as it necessitates higher energy input and additional treatment. The TEM analysis confirmed the achievement of the desired particle size with NGS exhibiting sizes below 20 nm.

The particle size plays a crucial role in determining the specific surface area. In the rubber compound, the interaction between the filler and rubber occurs both physically and chemically, predominantly at the surface of the rubber [13]. A higher surface area promotes stronger interaction between the filler and rubber, thereby determining the properties of the rubber product [21].

In accordance with ASTM D1765-21, the surface area values of NGS, as shown in Table 3, were within the category of high-grade fillers for rubber (>150 m^2/g). Silica with a larger surface area is advantageous for numerous applications [22].

On the other hand, the particle size distribution analysis still showed the presence of aggregate particles larger than 100 nm, contradicting to the observations from the TEM analysis. These results are consistent with the Ostwald ripening mechanism, as the reinforced silica aggregates are more resistant to breakage during the particle size analysis, indicating the measurements of aggregate size rather than primary particle size.

Table 3. Particle size distribution and surface area

Particle size distribution (nm)				BET surface area	Total pore volume
Avg D	D10%	D50%	D90%	(m^2/g)	(cc/g)
282.5	218.6	356.2	618.08	168.350	1.077

3.2. Bound rubber content

The bound rubber was analyzed using the rubber compound sheet as shown in Figure 2(a). Unlike carbon black, silica does not impart black color to the compound, making it easier to incorporate pigments and produce colorful products [9]. The silica aggregates are broken down and dispersed into the rubber matrix during the compounding process. The SEM image as illustrated in Figure 2(b) shows that the silica (bright white dots) readily fractures into smaller aggregates, resulting in a homogeneous rubber compound. The characteristics of the filler surface, the amount of filler added, and the degree of filler dispersion are significant factors determining the formation of bound rubber [23].

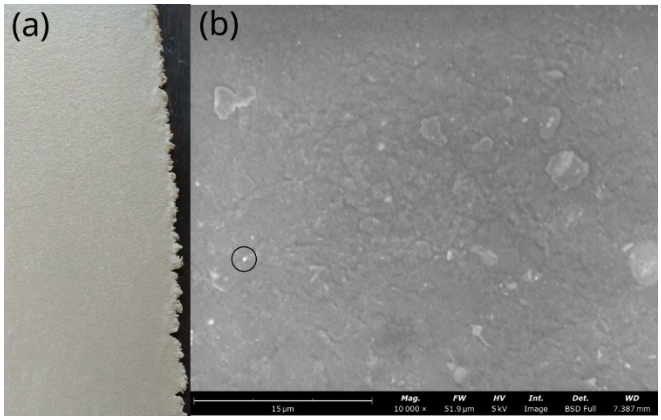

Fig. 2 Rubber composites (a) sheet and (b) SEM 10.000x

The analysis of the rubber compound involved the assessment of its bound rubber content (BRC) to evaluate the level of interaction achieved between the filler and rubber. BRC refers to the rubber bound to the filler's surface, either through physical or chemical means [13,23]. Figure (3) shows the correlation between silica loading and BRC.

Figure (3) demonstrates that an increase in filler loading led to a corresponding increase in the total, physical, and chemical BRC value. This relationship could be attributed to the larger number of active sites available for adsorption as more filler was added [23]. Thus, the potential for interaction with the rubber was enhanced. Furthermore, a higher filler content decreased the particle-to-particle distance, thereby facilitating the formation of inter-particle bridges. On the other hand, composites without added silica exhibited no bound rubber value due to the filler availability.

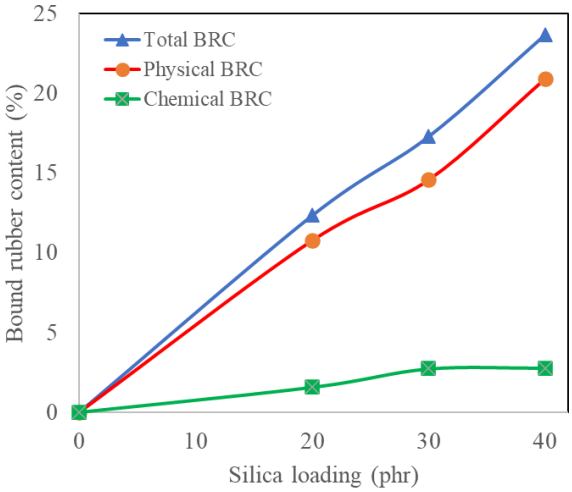

Fig. 3. Bound rubber content

Table. 4. Bound rubber content (BRC)

Filler loading	Total BRC	Fraction (%)	
(phr)	(%)	Physical BRC	Chemical BRC
0	0.00	0.00	0.00
20	12.34	87.30	12.69
30	17.29	84.27	15.72
40	23.68	88.31	11.68

Meanwhile, although the total BRC values may differ, the fraction ratio between chemical BRC and physical BRC in each sample was relatively constant, as shown in Table (4). The silica type utilized in these samples remaind the same, while the amount of filler varied. Hence, it can be inferred that the ratio of chemical and physical interaction between the rubber and filler was minimally affected by the quantity of filler added. The particle size of the filler contributed to the physical aspect, while the level of surface activity of the silica influenced the chemical contribution [24].

3.3. Rubber vulcanization characteristics

The moving dies rheometer was employed to monitor the transformations during the vulcanization process, which encompasses three stages: induction, curing or crosslinking, and overcure [24]. The analysis of vulcanization characteristics was conducted at 150°C using a rheometer as shown in Figure 4.

All rheometer curves of the rubber samples exhibited a similar pattern. The induction stage was characterized by a decrease in modulus, indicating the time at the vulcanization temperature where crosslink formation has not occurred until reaching the scorch time (ts_2) value. This was followed by the formation of crosslinks, as indicated by an increase in modulus. The process was determined by some factors such as the vulcanization temperature, type of rubber, and vulcanization system. As the vulcanization process proceeded, the amount of crosslinking agent and active sites diminished, resulting in a decrease in the reaction rate until the optimum modulus time (t_{90}) was reached. Further heating led to three possible overcure stages: an increase in vulcanizate stiffness (marching modulus), stability, or softening (reversion), dependent upon the type of

rubber [25]. Generally, the use of natural rubber reduces the vulcanization time, while thermal stability during overcure is provided by polybutadiene rubber [26]. In Figure (4), it can be observed that after t_{90} there was only a slight decrease in the modulus, therefore the rubber vulcanization had a relatively good thermal stability. The decrease in modulus often occurs at vulcanization temperatures above 140°C due to the partial breakage of polysulfide bonds [26,27].

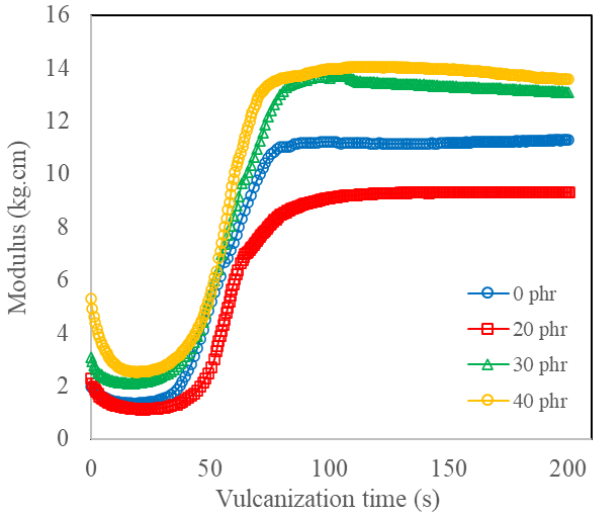

Fig. 4. Rheograph of rubber composite at various filler loading

Table 5. The cure characteristics of rubber compound

Silica loading (phr)	ML (kg.cm)	MH (kg.cm)	ts_2 (s)	t_{90} (s)	CRI (min^{-1})
0	1.22	10.21	12.80	120.20	55.87
20	1.24	8.88	19.50	83.00	94.49
30	2.36	15.44	12.20	70.80	102.39
40	2.61	18.61	14.00	78.70	92.74

The production of rubber compounds requires a balance between these three stages of the process. Sufficient scorch time (ts_2) is needed to avoid excessively long curing time, which would decrease production output. However, it should not be too fast to allow enough time for the compound to fill the mold cavity before it hardens due to crosslink formation [24]. Unlike most thermoset polymers, the crosslink density in rubber compounds changes very slowly during the induction stage [27].

From Table (5), silica loading with 20 phr provided the longer scorch time compared to rubber compound without filler. In the presence of silica, activators such as zinc oxide may be adsorbed and the accelerator system deactivated due to the absorption of moisture on the hydrophilic silica surface, thus leading to slower vulcanization initiation [10]. The polarity of silica attracts various chemicals, which also possess a number of polar characteristics [28]. This deactivation occurs when the accelerator is added to the rubber matrix after the silica filler, allowing for adsorption to take place. Interestingly, the scorch time decreased in the case of 30 phr, but then again increased to 40 phr. This phenomenon could be attributed to the presence of bound rubber. Bound rubber can cover a portion of the silica surface, thereby reducing its effectiveness in absorbing the activator.

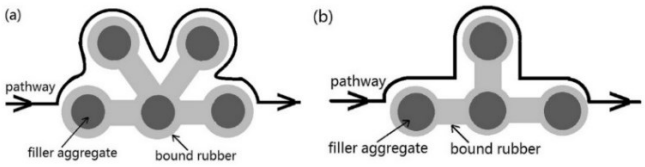

Fig. 5. Additives pathway (a) complex BRC (b) less complex BRC

On the other hand, the formation of bound rubber, could hinder the mobility of the additives, including the vulcanizing agents (sulfur, accelerator, and activator), particularly in the vicinity of the filler surface [23]. A higher amount of bound rubber, as depicted in Figure 5(b), resulted in a more complex interaction between the filler and rubber leading to the increasing hindrance compared to the lower amount as shown in Figure 5(a).

Table (5) also shows that the optimum curing time (t_{90}) and cure rate index (CRI) for rubber compounds with silica were faster than the sample without filler. Silica has the good thermal conductivity, which allows for better heat transfer during the vulcanization process [29,30]. This improves the heat transfer to promote faster and more uniform curing, leading to shorter cure times.

3.4. Swelling index and crosslink density

The crosslink formed in the rubber composite was determined through swelling tests and crosslink density calculations. The polymer chains in vulcanized rubber are typically not tightly packed [31], and there are some significant gaps within their molecular network. Naturally, natural rubber (NR), styrene-butadiene rubber (SBR), and polybutadiene rubber (BR) are the types of rubbers not resistant to oils [32]. Fig (6) illustrates the rubber composite's swelling value and crosslink density.

The addition of various additives can influence these inherent conditions, including the incorporation of fillers. Similarly, the vulcanization process of rubber also reduces swelling due to the formation of crosslinking networks [9]. However, aggressive media can penetrate through these gaps, causing an increase in the volume and weight of the sample. This phenomenon is known as swelling in rubber. Figure (6a) clearly shows a noticeable rise in the swelling value as the immersion time in toluene increases. This increase continues until a certain point, reaching the maximum swelling limit [10]. From Figure 6(b), the effect of the filler loading on the crosslink density was clearly shown. The crosslink density value corresponds to the data on bound rubber formation presented in Table 4. The overall crosslink density is influenced by the interaction between the filler and rubber, including the formation of monosulfide, disulfide, and polysulfide bonds [15]. Therefore, it is not surprising that in Figure 6(a), a higher crosslink density corresponded to a lower swelling index, indicating that the rubber composites were more resistant to solvent penetration and exhibited better stability.

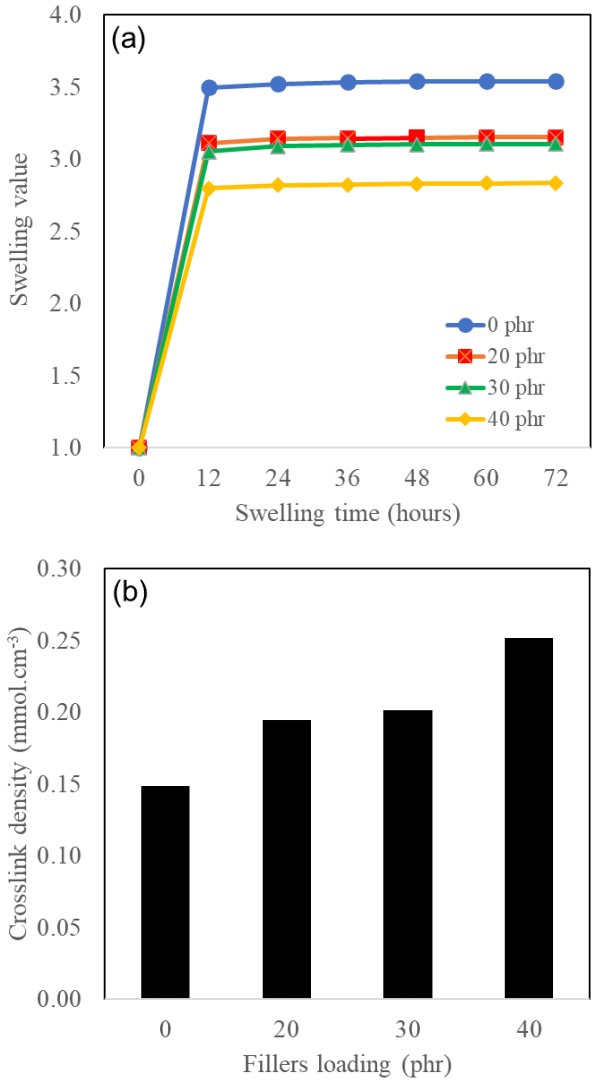

Fig. 6. Properties of rubber (a) swelling value (b) crosslink density

Table 6. Rubber crosslink density

Filler loading (phr)	Swelling index	Crosslink density (mmol/cm^3)
0	3.5398	0.1486
20	3.1516	0.1946
30	3.1052	0.2015
40	2.8329	0.2517

3.5. Rubber composite mechanical properties

The influence of silica loading on the mechanical properties of the vulcanized rubber samples was examined. Table 7 displays the measurements of hardness, elongation at break, tensile strength, and reinforcement index (RI) for the samples.

The hardness and elongation at break values of the samples increased with an increasing amount of filler used. The rise in value can be attributed to the higher interaction that can be established between the filler and rubber [15]. These findings aligned with the increased crosslink density observed when a greater quantity of filler was present, as indicated in Table 6. The formed rubber network structure became more complex, resulting in a higher level of hardness. The polymer chains in the rubber intertwined due to the presence of chemical crosslinking, which also contributed to higher elongation at break values within the observed filler's loading range. However, it is important to note that there is a limit to the amount of filler that can be used, especially beyond 40 phr, as a higher quantity of filler can reduce the softness of the rubber.

Meanwhile, the tensile strength and RI values showed an increase up to the addition of 30 phr of silica, followed by a decrease. A similar finding was also noted regarding the decline in tensile strength following a specific filler content [10,11]. This increase was the indicative of the presence of a rigid phase within the polymer matrix [28]. After 30 phr loading, the decrease may be attributed to the elevated difficulty in dispersing the filler at higher amounts due to silica aggregation caused by its polarity. The reformed aggregates can create weak points in the rubber, resulting in a decrease in its tensile strength [15].

Table 7. Rubber composite mechanical properties

Mechanical Properties	Silica loading (phr)			
	0	20	30	40
Tensile strength (kg/mm^2)	0.1927	0.2210	0.6548	0.5339
M100 (kg/mm^2)	0.1113	0.1444	0.1702	0.2298
M300 (kg/mm^2)	0.1895	0.2121	0.3710	0.3452
RI (%)	170.16	147.10	217.15	149.91
Elongation at break (%)	233.55	205.28	571.78	770.53
Hardness (Shore A)	48.00	56.50	59.50	62.50

4. Conclusion

The nanoparticle silica synthesized from geothermal waste had a primary size under 20 nm and a surface area of 168 m^2/g. The loading of silica in rubber composite was varied from 0 to 40 phr. The addition of silica into rubber composites led to an increase in the amount of bound rubber. Improved bound rubber formation influenced the mechanical properties and vulcanization characteristics in rubber composites. Mechanical properties such as tensile strength showed more than threefold as the loading increased from 0 phr to 30 phr followed by a slight decline at 40 phr loading.

When considering vulcanization characteristics, the addition of 20 phr of silica to the rubber resulted in an extended scorch time compared to the filler-free compound. The presence of silica allowed for the absorption of activators and accelerators, thereby delaying the initiation of vulcanization. However, the scorch time decreased after reaching 30 phr of silica loading. This decrease can be attributed to the higher amount of bound rubber covering a portion of the silica surface, thus reducing its ability to absorb the activator. Furthermore, silica possessed the good thermal conductivity, therefore facilitating the improved heat transfer during the vulcanization process and leading to shorter curing times. Overall, the findings indicated that a silica loading of 30 phr achieved a desirable balance between mechanical properties and vulcanization characteristics.

Acknowledgments

This work was supported by the Doctorate Dissertation

Grant No. 1935/UN1/DITLIT/Dit-Lit/PT.01.03/2022 from Universitas Gadjah Mada. The author also gratefully acknowledges the Rubber Workshop and Polymer Laboratory at Politeknik ATK Yogyakarta for technical support.

References

1. S. N. A. Jenie, A. Ghaisani, Y. P. Ningrum, A. Kristiani, F. Aulia, and H. T. M. B. Petrus, *Preparation of silica nanoparticles from geothermal sludge via sol-gel method*, AIP Conf Proc., 2026 (2018) 020008.
2. S. J. Zarrouk, B. C. Woodhurst, and C. Morris, *Silica scaling in geothermal heat exchangers and its impact on pressure drop and performance: Wairakei binary plant, New Zealand*, Geothermics, 51 (2014) 445–459.
3. J. A. Villarias, M. L. H. Yorro, M.-I. K. N. Galvan, and L. J. L. Diaz, *High Purity Silica Nanoparticles from Geothermal Waste Brine as Reinforcing Filler in Rubber Composite Material*, Mater. Sci. Forum, 894 (2017) 104–108.
4. S. Silviana, G. J. Sanyoto, A. Darmawan, and H. Sutanto, *Geothermal Silica Waste as Sustainable Amorphous Silica Source for The Synthesis of Silica Xerogels*, Rasayan J. Chem., 13 (2020) 1692–1700.
5. M. W. Syabani, I. Amaliyana, I. Hermiyati, and Y. I. Supriyatna, *Silica from Geothermal Waste as Reinforcing Filler in Artificial Leather*, Key Eng. Mater., 849 (2020) 77–83.
6. R. Sharafudeen, J. Al-Hashim, M. Al-Harbi, A. Al-Ajwad, and A. Al-Waheed, *Preparation and Characterization of Precipitated Silica using Sodium Silicate Prepared from Saudi Arabian Desert Sand*, Silicon, 9 (2017) 917–922.
7. J. Puskas, K. Chiang, and B. Barkakaty, *Chemistry, Manufacture and Applications of Natural Rubber*, Cambridge, UK: Woodhead Publishing, 2014.
8. S. Sattayanurak, J. W. M. Noordermeer, K. Sahakaro, W. Kaewsakul, W. K. Dierkes, and A. Blume, *Silica-Reinforced Natural Rubber: Synergistic Effects by Addition of Small Amounts of Secondary Fillers to Silica-Reinforced Natural Rubber Tire Tread Compounds*, Adv. Mater. Sci. Eng., 2019 (2019) 1–8.
9. M. W. Sya'bani, Y. Suwarno, M. F. Agustian, I. Perdana, and Rochmadi, *Studies of Geothermal Silica as Rubbers Compounds Reinforcing Filler*, AIP Conference Proceedings, 2217 (2020) 030144–1.
10. H. Sridharan, A. Guha, S. Bhattacharyya, A. K. Bhowmick, and R. Mukhopadhyay, *Effect of Silica Loading and Coupling Agent on Wear and Fatigue Properties of a Tread Compound*, Rubber Chem. Technol., 92 (2019) 326–349.
11. J. W. ten Brinke, *Silica Reinforced Tyre Rubbers: Mechanistic Aspects of the Role of Coupling Agents,* Ph.D. Thesis, Twente University, The Netherlands, 2002.
12. M. W. Syabani, R. Rochmadi, I. Perdana, and A. Prasetya, *FTIR study on nano-silica synthesized from geothermal sludge*, AIP Conf Proc., 1 (2022), Vol. 2440, p. 030014.
13. S. S. Sarkawi, W. K. Dierkes, and J. W. M. Noordermeer, *Elucidation of filler-to-filler and filler-to-rubber interactions in silica-reinforced natural rubber by TEM Network Visualization*, Eur. Polym. J., 54 (2014) 118–127.
14. S. S. Sarkawi, W. K. Dierkes, and J. W. M. Noordermeer, *Morphology of Silica-Reinforced Natural Rubber: The Effect of Silane Coupling Agent*, Rubber Chem. Technol., 88 (2015) 359–372.
15. D. Y. Kim, J. W. Park, D. Y. Lee, and K. H. Seo, *Correlation between the Crosslink Characteristics and Mechanical Properties of Natural Rubber Compound via Accelerators and Reinforcement*, Polymers, 12 (2020) 1-14.
16. R. Joseph, K. E. George, D. J. Francls, and K. T. Thomas, *Polymer-Solvent Interaction Parameter for NR/SBR and NR/BR Blends*, Int. J. Polym. Mater. Polym. Biomater., 12 (1987) 29–34.
17. A. Lazaro, N. Vilanova, L. D. Barreto Torres, G. Resoort, I. K. Voets, and H. J. H. Brouwers, *Synthesis, Polymerization, and Assembly of Nanosilica Particles below the Isoelectric Point*, Langmuir, 33 (2017) 14618–14626.
18. A. Lazaro, M. C. van de Griend, H. J. H. Brouwers, and J. W. Geus, *The influence of process conditions and Ostwald ripening on the specific surface area of olivine nano-silica*, Microporous Mesoporous Mater., 181 (2013) 254–261.
19. C. N. Suryawanshi, P. Pakdel, and D. W. Schaefer, *Effect of drying on the structure and dispersion of precipitated silica*, J Appl Crystallogr, 36 (2003) 573–577.
20. M. Sholeh, R. Rochmadi, H. Sulistyo, and B. Budhijanto, *Synthesis of precipitated silica from bagasse ash as reinforcing filler in rubber*, IOP Conf. Ser.: Mater. Sci. Eng. 778 (2020) 012012.
21. K. Ahmed, S. S. Nizami, and N. Z. Riza, *Reinforcement of natural rubber hybrid composites based on marble sludge/Silica and marble sludge/rice husk derived silica*, J. Adv. Res., 5 (2014) 165–173.
22. L. M. Quynh, H. V. Huy, N. D. Thien, L. T. C. Van, and L. V. Dung, *Synthesis of Si/SiO2 core/shell fluorescent submicron-spheres for monitoring the accumulation of colloidal silica during the growth of diatom Chaetoceros sp.*, Commun. Sci. Technol., 7 (2022) 1–7.
23. L. Song, Z. Li, L. Chen, H. Zhou, A. Lu, and L. Li, *The effect of bound rubber on vulcanization kinetics in silica filled silicone rubber*, RSC Adv. 6 (2016) 101470–101476.
24. M. Morton, ed., *Rubber Technology*, Doordrech, Netherlands: Springer Science & Business Media, 1999.
25. A. Ciesielski, *An Introduction to Rubber Technology,* Shawbury, UK: Rapra Technology Ltd., 1999.
26. G. Milani and F. Milani, *Comprehensive kinetic numerical model for nr and high-cis poly-butadiene rubber blends*, Chem. Eng. Trans., 57 (2017) 1495–1500.
27. G. Milani, E. Leroy, F. Milani, and R. Deterre, *Mechanistic modeling of reversion phenomenon in sulphur cured natural rubber vulcanization kinetics*, Polymer Testing, 32 (2013) 1052–1063.
28. J. Ramier, L. Chazeau, C. Gauthier, L. Guy, and M. N. Bouchereau, *Influence of Silica and its Different Surface Treatments on the Vulcanization Process of Silica Filled SBR*, Rubber Chem. Technol., 80 (2007) 183–193.
29. T. Mahrholz, J. Stängle, and M. Sinapius, *Quantitation of the reinforcement effect of silica nanoparticles in epoxy resins used in liquid composite moulding processes*, Compos. Part A Appl. Sci. Manuf., 40 (2009) 235–243.
30. M. Amin, A. Khattak, and M. Ali, *Influence of Silica (SiO2) Loading on the Thermal and Swelling Properties of Hydrogenated-Nitrile-Butadiene-Rubber/Silica (HNBR/Silica) Composites*, Open Eng., 8 (2018) 205–212.
31. X. R. Lu, H. M. Wang, and S. J. Wang, *Effect of swelling nitrile rubber in cyclohexane on its ageing, friction and wear characteristics*, Wear, 328–329 (2015) 414–421.
32. A. O. Patil and T. S. Coolbaugh, *Elastomers: A Literature Review with Emphasis on Oil Resistance*, Rubber Chem. Technol., 78 (2005) 516–535.